Available online at www.sciencedirect.com
SCIENCE DIRECT®
Journal of Nuclear Materials 349 (2006) 83–95
journal of nuclear materials
www.elsevier.com/locate/jnucmat

The texture dependence of K_{IH} in Zr–2.5%Nb pressure tube materials

SungSoo Kim *

Department of Nuclear Materials Technology, Korea Atomic Energy Research Institute, P.O. Box 105, Yousung-Ku, Taejon 305-353, Republic of Korea

Received 28 July 2005; accepted 27 September 2005

Abstract

The effects of the texture on the threshold stress intensity factor for a delayed hydride cracking (DHC: K_{IH}) along the radial direction was investigated for Zr–2.5%Nb CANDU pressure tube materials. The K_{IH} of the specimen with the highest basal pole component (F) for the cracking plane appeared to be the lowest K_{IH}, ~9 MPa $\sqrt{m}$, whereas that with the lowest F was over 20 MPa $\sqrt{m}$. The K_{IH} at 250 °C decreased linearly with F for the cracking plane. The texture dependence of K_{IH} on F was compared with the results from the literature, and the comparison appeared to be consistent. This dependence of K_{IH} can be explained by the rule of a mixture, as proposed in a previous work. It is concluded that the K_{IH} is predominantly determined by the F for the cracking plane and it is subsequently affected by the cracking direction. Why the texture dependence of K_{IH} in the radial direction occurs is discussed.

PACS: 62.20.mk

1. Introduction

The Zr–2.5%Nb pressure tubes in CANDU reactors have suffered primary coolant leakage accidents in the rolled joint region due to the mechanism of a delayed hydride cracking (DHC) since the 1970s [1]. It is understood that the DHC crack grows by a repeated process of both precipitation and fracture of the hydride at the crack tip when the hydrogen concentration exceeds the terminal solid solubility (TSS) at the temperature of concern [2]. The DHC velocity (DHCV) and the threshold stress intensity factor (K_{IH}) are important parameters for an evaluation of the integrity of the reactor, because these properties can be used to determine whether stable crack growths start or not and to predict when the growing crack will reach the critical crack length (CCL).

A study on the effect of texture variation on the DHC behavior has confirmed that the DHCV increases exponentially with a basal pole component (F) for the cracking plane and that K_{IH} decreases linearly with F in the Zr–2.5%Nb plate [3]. It has been shown that the texture dependence of K_{IH} is valid for various Zr-alloy plates and tubes using the results reported in the literatures [4–7], as shown in Fig. 1 [3].

* Tel.: +82 42 868 2061; fax: +82 42 868 8346.
E-mail address: sskim6@kaeri.re.kr

0022-3115/$ - see front matter © 2005 Elsevier B.V. All rights reserved.
doi:10.1016/j.jnucmat.2005.09.027

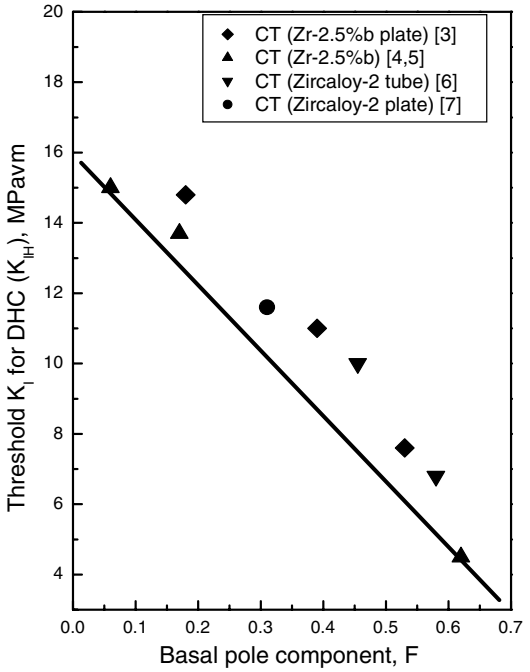

Fig. 1. Threshold stress intensity factor (K_{IH}) with a basal pole component (F) [3].

The basal pole component, F, which is the resolved fraction of the basal planes in the selected direction, is calculated by the method proposed by Evans et al. [8] and Winegar [9]. The basal pole component is defined by Eq. (1):

$$F = \sum V_\alpha \cos^2 \alpha, \tag{1}$$

where α is the angle between the basal pole of the grain and the direction of interest, and V_α is the volume fraction of the grains tilted at angle α.

The increasing DHCV trend with F was explained by a preferred precipitation of the hydride for the cracking plane, and the decreasing behavior of the K_{IH} with F was explained by the rule of a mixture using F as a fraction of the brittle matter and $(1 - F)$ as a ductile matrix [3].

Furthermore, the lowering effect of F on K_{IH} was confirmed by the experimentally fabricated Zr–2.5%Nb tube, called the radial textured tube, having a higher F in the radial direction ($F_R = 0.48$) and a lower F in the transverse direction ($F_T = 0.32$) of the tube, when compared to the commercial CANDU pressure tube ($F_R = 0.33$ and $F_T = 0.59$), as shown in Fig. 2 [10].

The anisotropy of the DHC behavior has been reported by Sagat et al. for the DHCV in the longitudinal direction as being about two times faster than that in the radial direction in certain temperature ranges [2]. Two different cracking modes are illustrated in Fig. 3 [2]. It is reported that the K_{IH}'s of the cantilever beam (CB) specimens in the radial direction are about 50% greater than that of the curved compact tension (CCT) specimens, where the crack grows in the longitudinal direction [12]. These results suggest that the cracking direction affects the DHC behavior.

The aim of this study is to understand the effects of the texture on the K_{IH} along the radial direction through a texture variation in Zr–2.5%Nb pressure tube materials, and to present the trend of the texture dependence of K_{IH}, because both have not yet been studied. The results of this study may be used as a trend of the K_{IH} for a flaw assessment in the evaluation of the integrity of a pressure tube

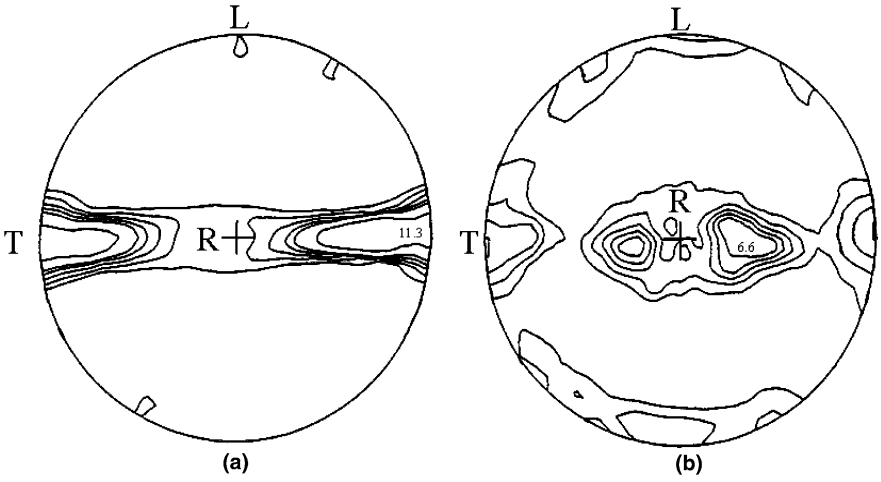

Fig. 2. (0002) pole figures for: (a) commercial CANDU pressure tube and (b) radial textured tube [10].

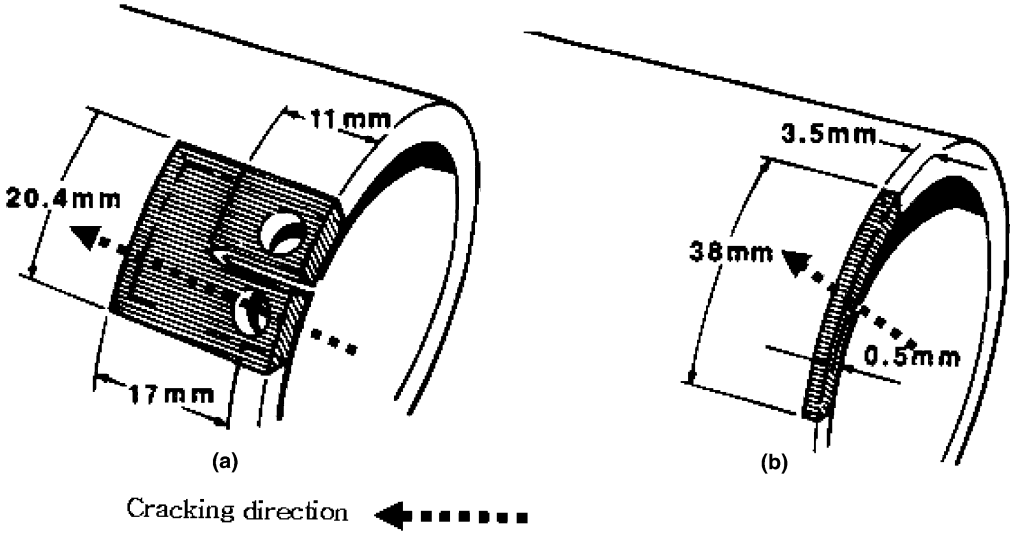

Fig. 3. Schematic illustration of two different delayed hydride cracking (DHC) modes in a CANDU pressure tube [2]. (a) A curved compact tension (CCT) (T–L); (b) a cantilever beam (CB) (T–R).

containing inclined flaws from the axial–radial plane, when the crack grows in the radial direction.

2. Experimental

In order to investigate the effect of the texture on K_{IH} along the radial direction in Zr–2.5%Nb pressure tube materials, it is necessary to acquire specimens with various textures for the cracking plane and with a minimum change of the microstructure.

The Zr–2.5%Nb pressure tube for the CANDU reactor is hot extruded and cold drawn by about 25%, and then, stress relieved for 24 h at 400 °C. The Zr–2.5%Nb pressure tube manufactured using a quadruple melting ingot for the CANDU reactor was flattened by the reverse bend method in order to obtain a plate-like material, since it is very difficult to carry out the K_{IH} tests along the radial direction without a flattening due to the tube geometry.

The reverse bending apparatus was a empirically designed by Chalk River Laboratories, which consisted of a short-large circular block with ~400 mm diameter × ~80 mm length and a small circular block (reverse roller) with a ~80 mm diameter × ~80 mm length. Both have a hole in the center for the assembly. The CANDU pressure tube for the reverse bend was cut to be about 60 mm long, since the maximum capability of a reverse bending should be smaller than 80 mm. Furthermore, the required force would be increased with the width. This tube was cut axially and it was drilled for a bolting so as not to be free during the reverse bending process, to a short-large circular block for a reverse bending. A small roller is inserted inside the tube for the reverse bend. Then, the short-large block and the smaller roller are assembled by additional rods at both sides, which allow the reverse bending action for the reverse bend. Then, the smaller roller is rolled on the short-large block manually until the tube is reversely flattened on the short-large block. Finally, the tube becomes a flattened tube, and, then, the flattened tube specimen is get ready.

The texture of the flattened material may be changed slightly, because the inside of the tube experiences a tensile strain, and vice versa. However, since the DHCV and K_{IH} measurement were carried out in the middle of the plate, it is expected that a slight change in the texture by a reverse bending has little effect on the results. In addition, the F was calculated from the measured inverse pole figure after a flattening and a stress relieving treatment.

The stress relieving treatment was conducted at 400 °C for 88 h to relieve the residual stress formed during the reverse bending process after the surface hydrides formed during the electrolytic hydrogen charging process in the sulfuric acid solution were ground off. However, this treatment simultaneously broke up the β-phase network between the grain boundaries of the discrete form. Although the breaking up of the β-phase network may affect the diffusion of hydrogen through the grain boundary, it will have little effect on the measurement of the effect of the texture on the DHC behavior in this

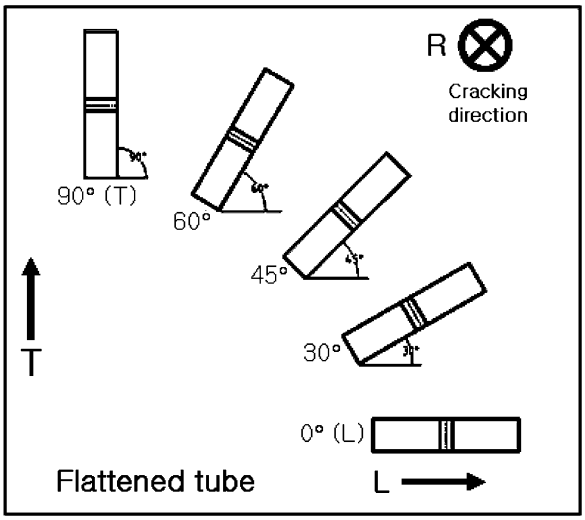

Fig. 4. Schematic illustration of a machining of cantilever beam (CB) specimen.

study, because the effect of the texture is determined by a matrix with a hexagonal close packed (HCP) crystal.

The texture variation was achieved by machining the CB specimens at various angles, as shown in Fig. 4. The specimens were machined at 0°, 30°, 45°, 60°, 90° from the longitudinal direction. The cracking directions of all the CB specimens were fixed in the radial direction and the machined side of the notch on the flattened tube was the outer side of the original tube. The dimensions of the specimens were 25.4 mm in length, 3.2 mm in width, and 4.2 mm in thickness.

The procedure of the K_{IH} tests and the hydrogen addition are described fully in the literature [11]. Fatigue pre-crack was introduced at the notch tip of the CB specimens using a three point bend grip and the final K_I at the crack tip was less than 15 MPa $\sqrt{m}$, since the initial K_I was selected as 17 MPa $\sqrt{m}$ according to the testing procedure. The formula for the calculation of K_{IH} is described in the literature [4]. The hydrogen content was analyzed as ~60 ppm and the K_{IH} tests were carried out at 250 °C.

The hydride morphology and the DHC fracture surface were observed with an optical microscope and scanning electron microscope (SEM). The inverse pole figures for the CB specimens with various textures were determined using CuK_α radiation and the F was calculated from the inverse pole figures [8,9].

3. Results

The morphology of the hydride varied with the tilting angle and changed slightly with the thickness, as shown in Fig. 5. These are the microstructures for the specimens after a homogenization. All the hydrides are aligned to be nearly parallel to the axial-circumferential plane and no radial hydride is seen in the microstructure because it is understood that the radial hydrides are precipitated during the DHC testing after a full dissolution during a soaking. Therefore, it is very difficult to observe the hydride in the axial-circumferential plane.

The inverse pole figures of the tilted CB specimens for the cracking plane are compared in Fig. 6. The (0002) and $(10\bar{1}0)$ poles are concentrated in the transverse direction and the longitudinal direction, respectively. It appears that F varied from 0.03 in the longitudinal direction to 0.64 in the transverse direction.

The K_{IH} measured at 250 °C are plotted against the basal pole components in Fig. 7, in which the tilted angles are plotted together. This temperature is considered to be a main concern for pressure tubes, because this temperature is the coolant inlet temperature in a CANDU reactor. It is known that a material with 60 ppm hydrogen, dissolves fully at 250 °C when it is cooled down from the proper soaking temperature for 1 h at 310 °C, however, this has a certain amount of hydride if the temperature is raised from room temperature without a soaking treatment. The K_{IH} values decreased linearly with an increase in F. The K_{IH} with the highest F ($F_T = 0.64$) at 90° showed the minimum values. The longitudinal CB specimens having the lowest F ($F_L = 0.03$) could not be cracked at all. It is possible to estimate that the K_{IH} for the longitudinal specimen can be considered to be over 20 MPa $\sqrt{m}$ when compared with the results of the 30° tilted CB specimens.

The macroscopic morphology of the pre-fatigue and DHC surfaces observed by a stereo microscope are compared in Fig. 8. The characteristics of the DHC surface in the tilted CB specimens except the 90° are that there are white-colored bands between the dark area by a DHC, marked by arrows in Fig. 8(b)–(d). In addition, the spacing of the band is decreased with a decrease in the tilting angle and F. However, the DHC did not occur in the 0° (L) tilt specimen (Fig. 8(e)).

The DHC surfaces observed by SEM are shown in Fig. 9. It is clear that the DHC surfaces in the

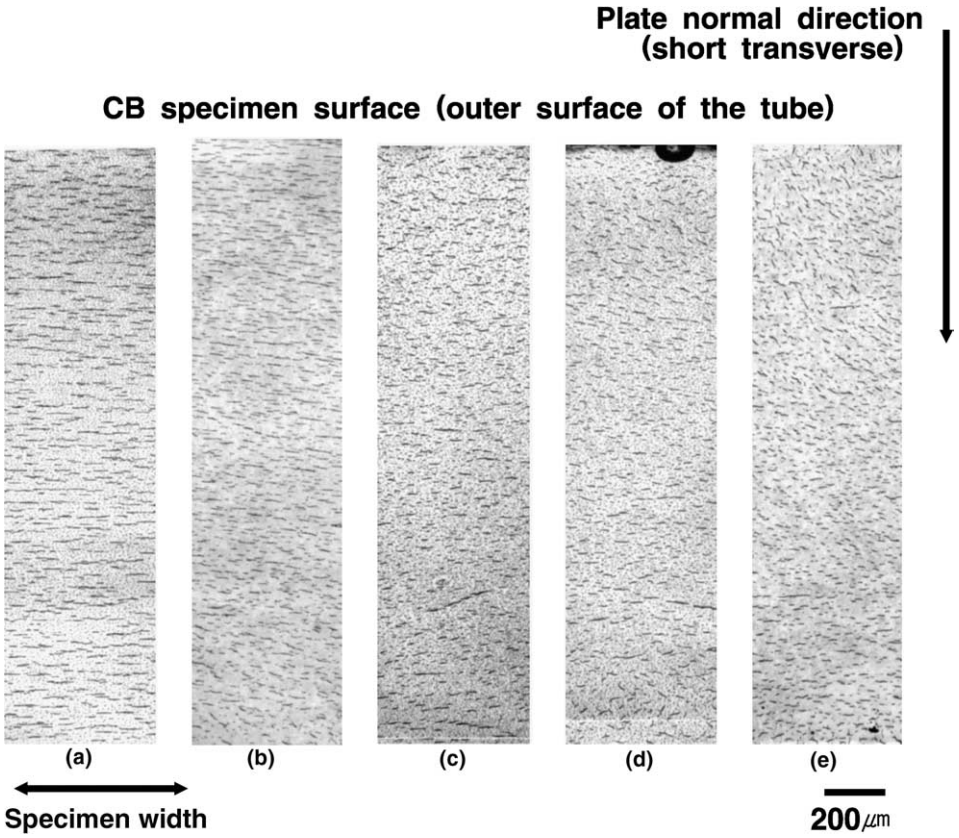

Fig. 5. Hydride morphology for a half thickness of the tilted CB specimens: (a) 90° (T), (b) 60°, (c) 45°, (d) 30°, and (e) 0° (L) CB.

60°, 45°, and 30° tilted specimens (Fig. 8(b)–(d)) are very bumpy and show some chunky-wedges, whereas the surface in the 90° specimen is relatively smooth. The white-colored bands in Fig. 8(b)–(d) are chunky-wedges in Fig. 9(b)–(d), and these are the un-cracked ligaments connected to the opposite cracking plane as bridges during a DHC, even though the DHC occurs through the susceptible grains. These provide an additional load enduring mechanism. These are broken during the fracturing process after a DHC for the evaluation procedure. This is a freshly-cracked surface whereas the DHC surface is oxidized to a dark blue or brown color.

The microscopic DHC surfaces are compared in Fig. 10. This shows that the cracking process can be changed significantly with the texture in the cracking plane. The degree of the bumpiness increased with the F and a decrease in the tilting angle. It seems to be due to the fact that the habit plane of the hydride precipitation has inclined from the cracking plane pre-designed to be fractured and the plane having a higher F provides an easier path for the DHC. Therefore, the required energy to propagate the DHC crack and the K_{IH} will be increased with a decrease in F for the cracking plane.

4. Discussions

It was possible to investigate the effects of the texture on the K_{IH} with a minimum change in the specific pressure tube microstructure. The minor changes in the microstructure are the decomposition of the β-phase and the shape of the grains for the cracking plane since the grains were elongated in the longitudinal direction. However, these microstructural changes will not vary the K_{IH}, significantly, since the DHC process would be mainly controlled by the property of the matrix.

The linear dependence of K_{IH} on F is shown in Fig. 7 in the range of $F = 0.19$–0.64 (Fig. 6(b), (d), (e) and (f)). This trend is consistent with the literature [3], except the level of the value. The results obtained in Zircaloy-2 and Zr–2.5%Nb are plotted together against the F in Fig. 11 [3–7,10,11], this shows that there is a significant texture dependence

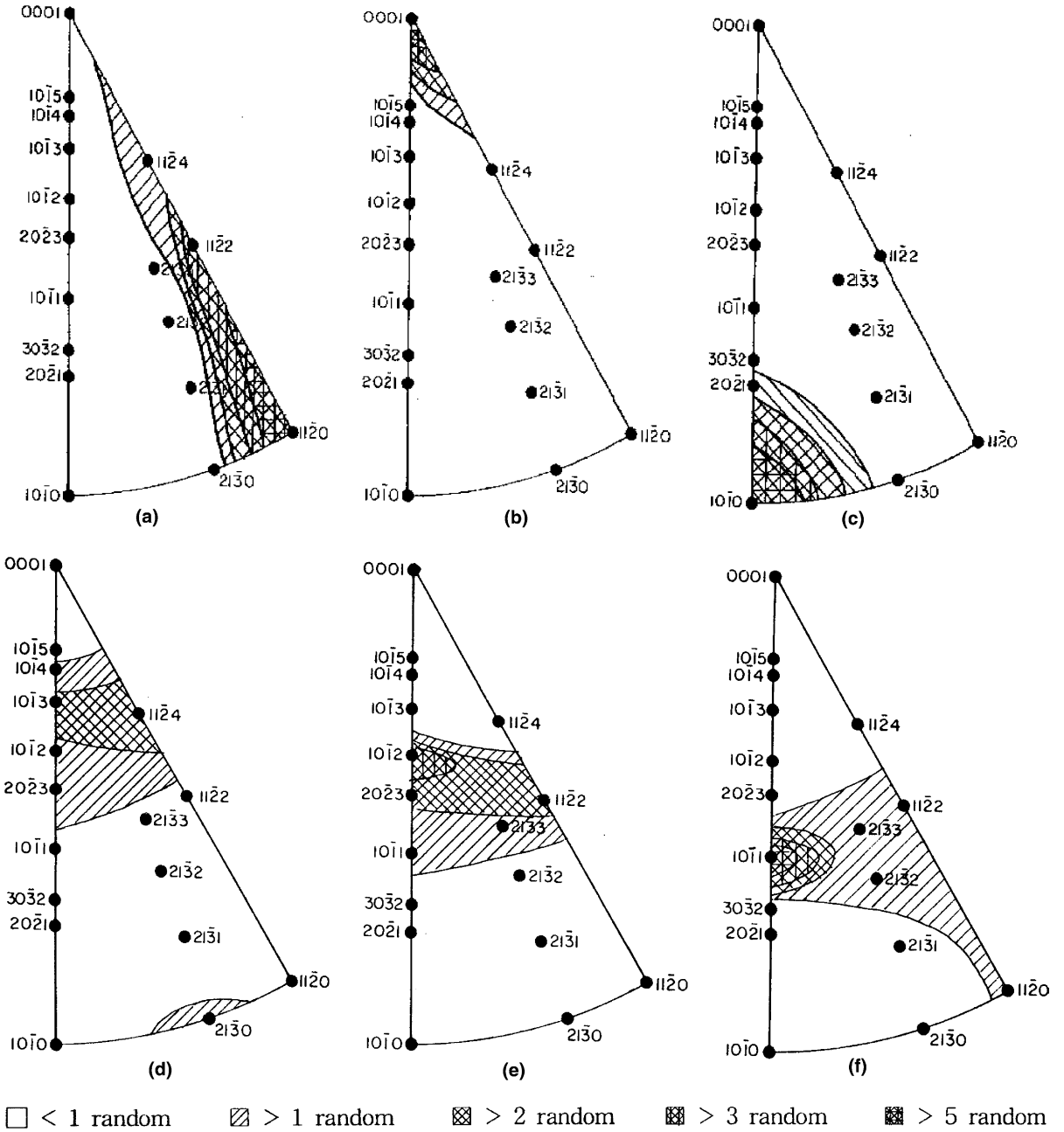

Fig. 6. Inverse pole figures in the plane normal to the cracking plane for the tilted CB specimens taken from the flattened material: (a) plate normal (radial (R), $F = 0.27$); (b) 90° (T), $F = 0.64$; (c) 0° (L), $F = 0.03$; (d) 60°, $F = 0.41$; (e) 45°, $F = 0.30$ and (f) 30° Tilt, $F = 0.19$ (random means average texture coefficients).

regardless of the materials. This is due to the fact that the major phase is α-Zr in both the materials.

The K_{IH} is a critical K_I value over which the crack grows physically through the DHC mechanism. The DHC mechanism involves the kinetics of the formation of the hydride, namely, the diffusion of hydrogen to the crack tip region and the precipitation of the hydride and its fracture under the given loading condition. When the applied load is constant, then the applied K_I at the crack tip will be constant. Only the precipitation of the hydride at the crack tip will be changed with time. The load enduring capability will be decreased with an increased fraction of the hydride at the crack tip.

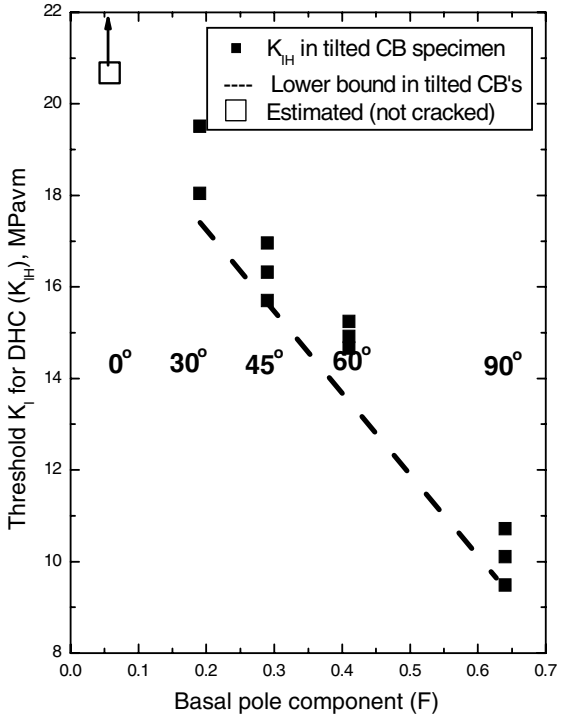

Fig. 7. The dependence of F in the cracking plane of the K_{IH} in the tilted CB specimens.

If the applied load or stress at the crack tip exceeds the load enduring capability with the aid of the hydride at the crack tip, a certain length of the mixture of the hydride and matrix will be fractured simultaneously, and this process will be repeated. This is the very mechanism of a DHC. Therefore, there might be inherent K_{IH} values of a given texture, according to the distribution of the basal planes or the habit plane of the hydride, $(10\bar{1}7)$ [13].

The relationship between the most probable habit planes of the hydride and the cracking planes in the titled CB specimens is shown in Fig. 12. This clearly shows the role of the habit plane of the hydride during a DHC. The interplanar angle between the cracking plane of the 90° CB specimen and the habit plane of the hydride is ~15° in both habit planes 1 and 2, $(10\bar{1} \pm 7)$. The crack of the 90° (T) CB specimens propagates in both habit planes 1 and 2 in Fig. 12. This is the reason why the DHC surfaces in Fig. 8(a), Fig. 9(a), and Fig. 10(a) are relatively smooth.

However, the crack of the 45° tilted CB specimens in Fig. 12 propagates through habit plane 1 only, because the interplanar angle between the cracking plane of the 45° CB specimen and habit plane 1 is ~30° but that for habit plane 2 is ~ 60°. It is natural, that the one closer to the cracking plane is activated since the tensile stress is greater. In the case of the 0° specimens ($F_L = 0.03$), the interplanar angle between the cracking plane of the 0° CB specimen and both habit plane 1 and 2 is ~75°. Therefore, there are almost no habit planes of the hydride near or parallel to the cracking plane. This is why the 0° CB specimens did not crack by a DHC at all, as shown in Fig. 8(e), Fig. 9(e), and Fig. 10(e).

The increase in F in the cracking plane reduces the area of the ductile matrix. This means that the plane having a higher F has a lower resistance to a DHC. Therefore, if F for the cracking plane is higher, then the K_{IH} is lower; the K_{IH} decreases with F, and vise versa. The increasing effect of F can be understand clearly, by referring to Fig. 9(a)–(d). This concept in the cracking plane for DHC can be illustrated by two dimensionally in Fig. 13.

The thickness of a plastically deformed region during DHC should be very thin because the fracture surface shows a little plastic deformation after DHC. Although this thickness is dependent on the applied in situ K_I, the load enduring concept by a ductile matrix can be shown easily as in Fig. 13. The area F can be treated as a void or a useless matter for load enduring state because the hydride can be precipitated into this region and the hydrides in this region provide not only a brittle characteristic but also an obstacle for dislocation motions in the plastic zone at the crack tip.

This behavior can be explained by the rule of a mixture [3]. The volume fraction of the ductile matrix can be assumed as $(1 - F)$ and that of the brittle hydride can be assumed as F, because the physical meaning of F is the resolved fraction of the basal plane in the cracking plane. The texture dependence of K_{IH} can be expressed by the following Eq. (2) [3]:

$$K_{\text{IH at } F} = (1 - F) \times K_{\text{IH of the hydrided matrix at } F=0} + F \times K_{\text{IC of Zr-hydride}}, \quad (2)$$

where $K_{\text{IC of Zr-hydride}}$ is the fracture toughness which is reported as $K_I = 1$–$3\ \text{MPa}\sqrt{\text{m}}$ [14], $K_{\text{IH of the hydrided matrix at } F=0}$ is the fracture toughness of a complete ductile matrix containing hydrogen at $F = 0$.

$K_{\text{IH of the hydrided matrix at } F=0}$ in the CT specimen can be estimated to be $\sim 16\ \text{MPa}\sqrt{\text{m}}$ in Fig. 1, but that in the CB specimen can be estimated to be $\sim 21\ \text{MPa}\sqrt{\text{m}}$ in Fig. 11, if extrapolated at $F = 0$. This shows that the $K_{\text{IH of the hydrided matrix at } F=0}$ varies according to the cracking direction. The physical meanings of these

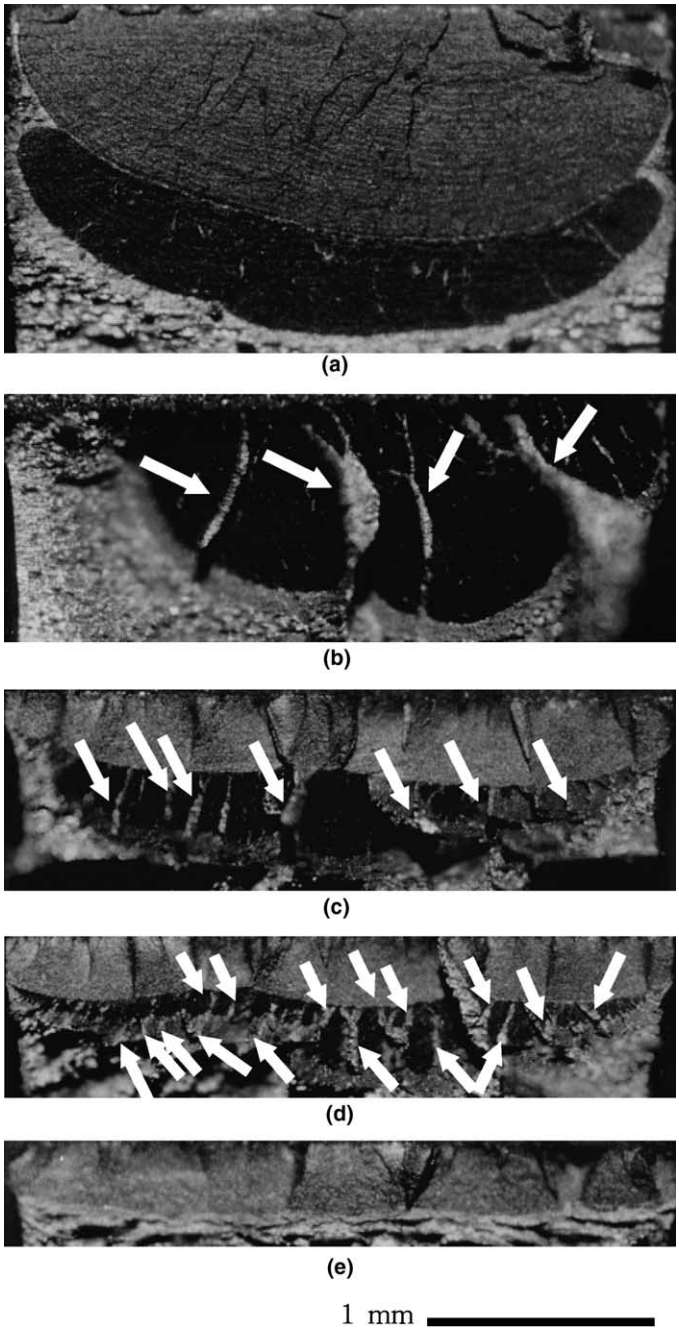

Fig. 8. Comparisons of the macroscopic morphology of the DHC surfaces by a stereo microscope in the tilted CB specimens: (a) 90° (T), (b) 60°, (c) 45°, (d) 30°, and (e) 0° (L) (arrows denote the un-cracked ligaments).

values are the maximum toughness (K_{IH}) of a matrix containing hydrogen to the DHC, in which there is no hydride parallel to the cracking plane. This would be a similar value in the 0° ($F_L = 0.03$) specimen in this study, although authors were not able to determine it properly in this study.

The K_{IH} decreases with F in both the cracking directions because the volume fraction of the

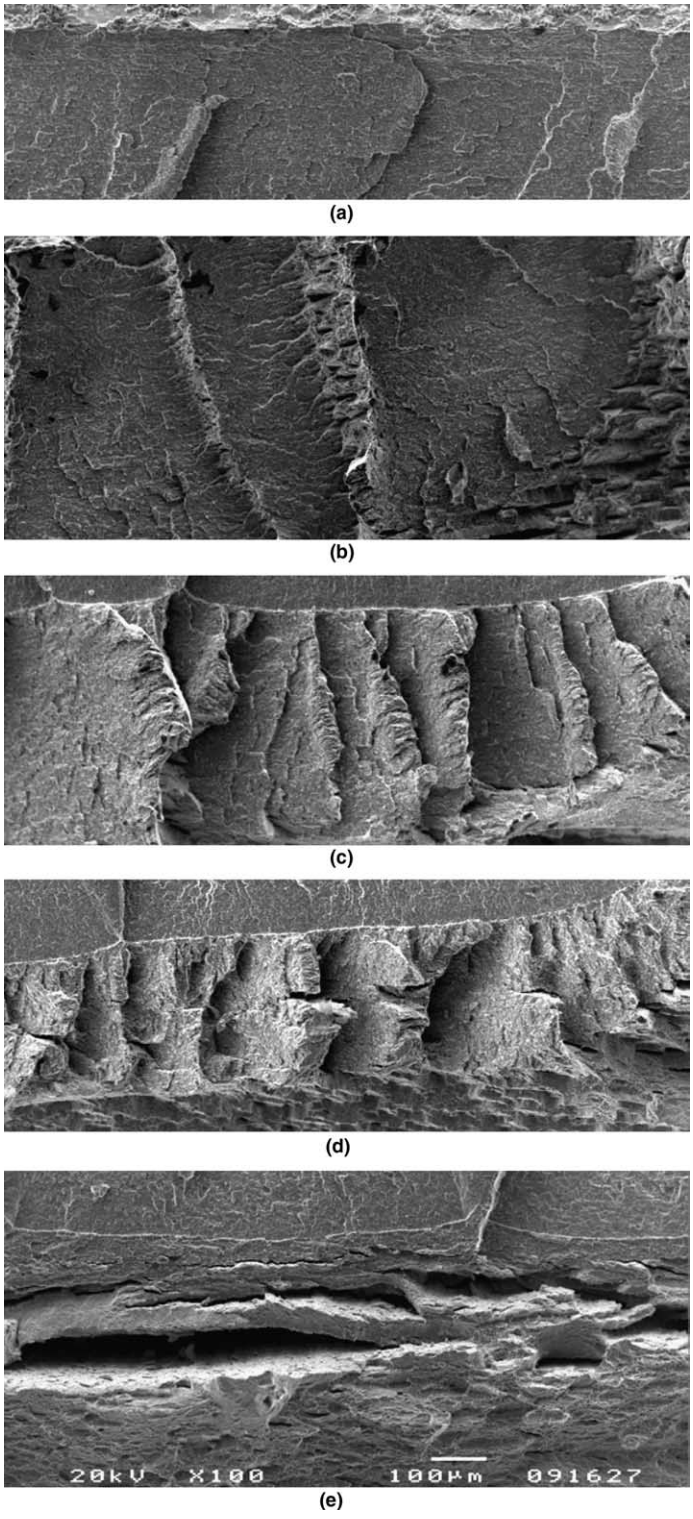

Fig. 9. Comparisons of the macroscopic morphology of the DHC surfaces by SEM in the tilted CB specimens: (a) 90° (T), (b) 60°, (c) 45°, (d) 30°, and (e) 0° (L).

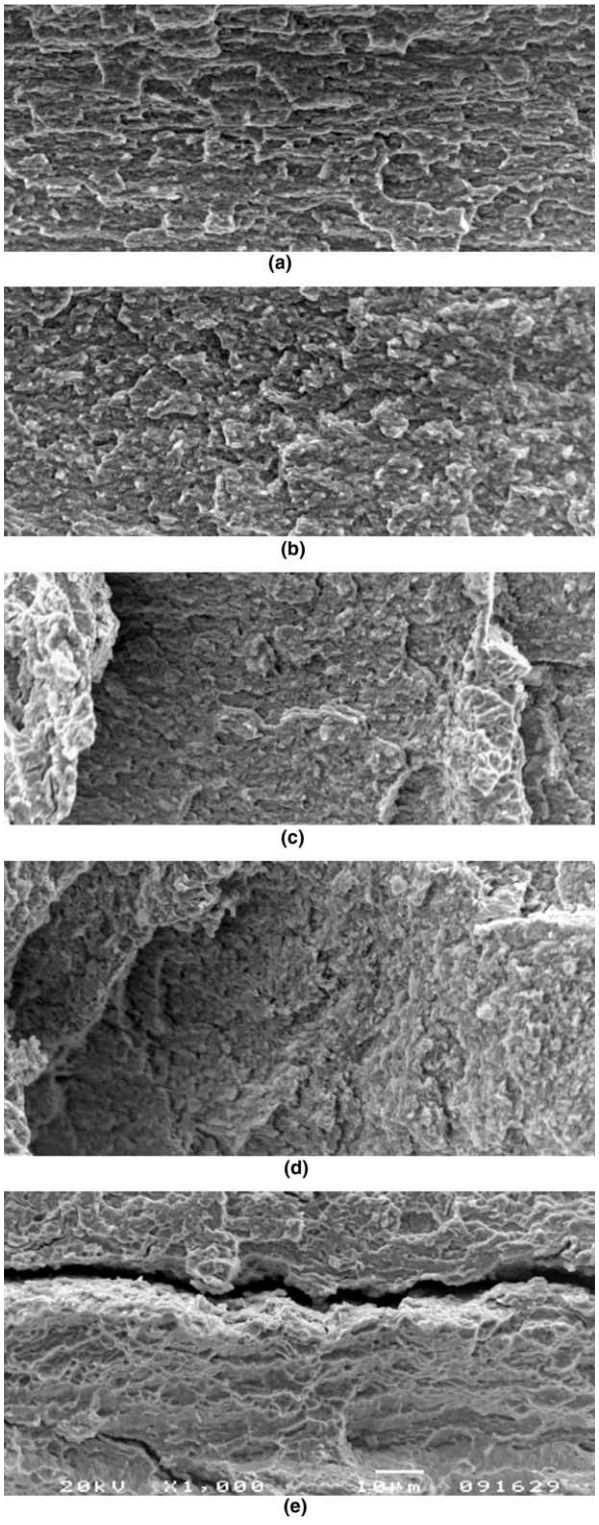

Fig. 10. Comparisons of the microscopic morphology of the DHC surfaces by SEM in the tilted CB specimens: (a) 90° (T), (b) 60°, (c) 45°, (d) 30°, and (e) 0° (L).

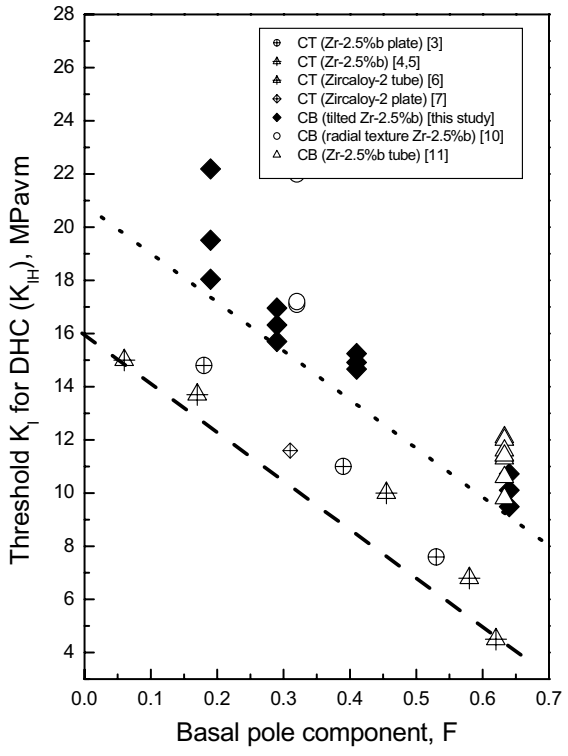

Fig. 11. The texture dependence of K_{IH} in the various Zr-alloys from the CCT (CT) and CB specimens.

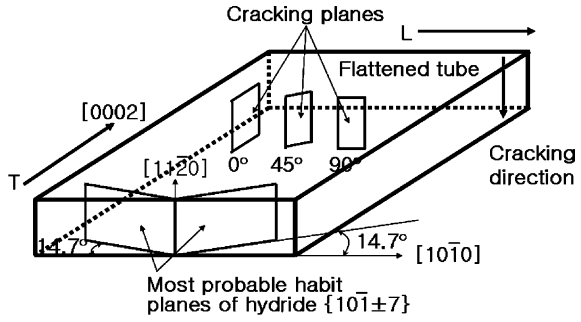

Fig. 12. Schematic illustration of the relationship between the most probable habit planes of the hydride and the cracking planes of the tilted CB specimens.

hydride increases with F, even though the fracture toughness of a complete ductile matrix containing hydrogen ($K_{IC\ of\ the\ hydrided\ matrix}$) is constant. The K_{IH} at $F = \sim 0.62$ in the CT and CB specimens are estimated to be $\sim 5\ MPa\sqrt{m}$ and $\sim 9\ MPa\sqrt{m}$, respectively. These values are much lower than that of the dynamic fracture toughness, $K_{IC} = \sim 25\ MPa\sqrt{m}$ at $F = 0.62$ [15–17]. This may be due to the characteristics of a DHC involving the kinetics of a hydride formation. Therefore, it can

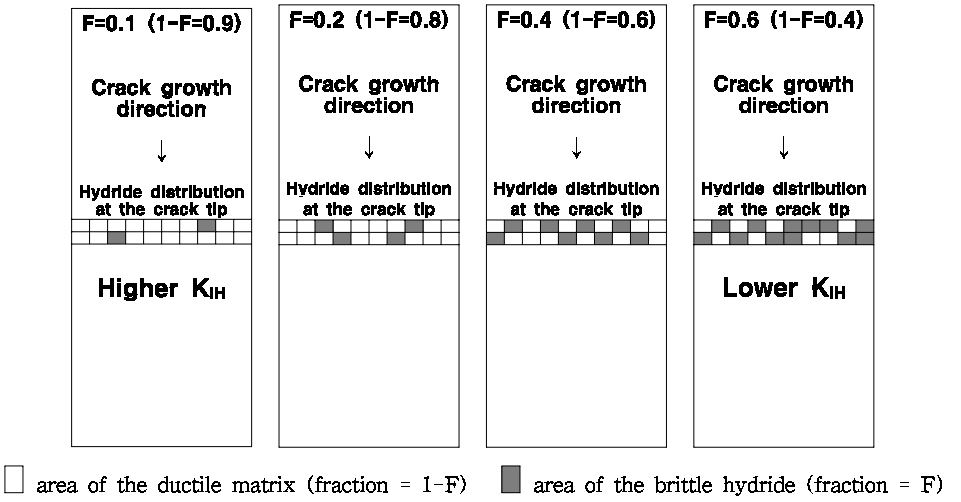

Fig. 13. Schematic illustration of the effects of the texture on K_{IH} at the crack tip region in the Zr–2.5%Nb material with F, composed of the brittle hydride (fraction: F) and the ductile matrix (fraction: $1 - F$).

be concluded that the concept of K_{IH} is totally different from that of K_{IC}.

The K_{IH}'s in the CB specimens in the transverse direction are about 50% higher than that of the CT specimens, as shown by the lower dashed line in Fig. 11. Even though the cracking plane is identical in the CB and CCT specimens except in the cracking direction, there are two different trends for the texture dependence of K_{IH}. This shows that not only F for the cracking plane but also the cracking direction is important. The basal poles in the CANDU pressure tubes are concentrated in the transverse direction and they are dispersed from the transverse to the radial direction within 40°. Therefore, there are certain differences in the grain orientations at the crack tip region, and, thus, it may cause a different cracking behavior.

Generally, the fracture toughness would be controlled by the accommodation capability of the plastic deformation due to a stress concentration at the crack tip. Therefore, the K_{IH} would be dependent on not only the toughness of the cracking plane but also on the cracking direction, as explained above. The directional DHC characteristic has been investigated through the XRD analysis of the DHC fracture surface and it is identified that the plastic deformation mechanisms operated during the DHC process were different between the CCT and CB specimens [18]. At least, it is confirmed that only $\{10\bar{1}2\}$ and both $\{10\bar{1}2\}$ and $\{11\bar{2}1\}$ twinning systems operated in the CCT and CB, respectively.

This is related to the grain orientations at the crack tip during cracking, although the average grain orientations in the cracking plane are the same. The grain orientations at the crack tip in the CB and CT specimens are aligned in the radial and longitudinal direction, respectively, as shown in Fig. 6. The grain orientations in the cracking direction in the CCT (or CT) specimen are mostly $[10\bar{1}0]$ and these are very close to each other along the longitudinal direction within 10–15° regardless of the orientation of the (0002) pole. However, those in the CB specimen vary from $[11\bar{2}0]$ to $[11\bar{2}4]$ via $[11\bar{2}2]$, and this means that the orientation of the neighboring grain may change significantly. This angular range is over 60° in the CB specimen. Since the grain orientations at the crack tip in the CB specimens have a considerable variation, when compared to the CT specimens, this may inhibit a cracking in the radial direction.

The material used in this study has been stress relieved for 88 h at 400 °C. Although this treatment has been selected in order to eliminate the effect of the hydrogen diffusion path through the β-phase network along the grain boundary, this treatment would provide a greater recovery or annealing effect [4]. Therefore, the difference in K_{IH} between the radial and the longitudinal direction might originate from the difference in the stress relieving treatment, because this stress relieving treatment might increase the accommodation capability, as discussed above.

On the other hand, it is known that the fracture toughness of the Zr–2.5%Nb CANDU pressure tube material is very sensitive to the content of chlorine (Cl) and that the chlorine content is controlled to be lesser than 1 ppm [12]. The materials used in

this study are made of a quadruple melted ingot. However, the materials used to obtain the K_{IH} from the CTs might have a higher chlorine content because the effect of the chlorine content on the fracture toughness in Zr–2.5%Nb alloy was not known at the time of manufacture and thus it could not be controlled during the manufacturing process. Therefore, the material made of a quadruple melted ingot has a relatively higher fracture toughness when compared to a double melted one, and this material might inherently have a fracture resistance. Thus, this fact seems to be the reason why the K_{IH}'s in this study are higher than that from the CTs.

The main concern of the DHC characteristics in the CANDU reactor is for the operating pressure tube [2]. It is well known that the irradiated pressure tube materials have a very low tensile elongation and fracture toughness. The degradation or deterioration of the pressure tube materials is understood to be due to various defects introduced by neutron irradiation, such as vacancies, vacancy clusters, vacancy loops and interstitial dislocation loop, etc. All these defects impede the slip or the motion of the dislocation. This is the main concept as to why the toughness and/or ductility is reduced by neutron irradiation. Therefore, the difference in K_{IH} between the radial and axial direction might be reduced, since the accommodation capability of the plastic deformation due to a stress concentration at the crack tip would be lost by irradiation regardless of the direction.

The hydrogen content in the DHC specimens is important because it determines the temperature at which a DHC occurs. The DHC testing at 250 °C would show the maximum DHC velocity for the specimen with 60 ppm of hydrogen. The soaking temperature, 310 °C, is chosen to dissolve the hydride fully into a solution for the specimen with 60 ppm of hydrogen in Zr–2.5%Nb alloy [2]. Therefore, it is expected that the maximum temperature at which a DHC occurs would be lowered if the hydrogen content is lowered. Furthermore, the specimen with less than 60 ppm of hydrogen would show a lower DHC velocity since there is a proper condition for the maximum DHC velocity, such as 60 ppm at 250 °C after a soaking at 310 °C.

The DHC fracture surface have been examined by XRD [18]. It was confirmed that there was a strong diffraction from the δ-hydride. It is reasonable that the hydride exists on the DHC fracture surface, because there is no reason for the hydride on the DHC fracture surface to dissolve.

Meanwhile, the longitudinal CB specimens were not cracked with and without a fatigue crack at the notch. Only a bending occurred without a fatigue crack, or the axial-circumferential cracking occurred, as shown in Fig. 8(e), Fig. 9(e), and Fig. 10(e). These micrographs in the longitudinal specimens show no DHC crack and show some axial-circumferential cracks near crack tip region. This is consistent with the explanation by the rule of a mixture, i.e. it is very difficult to propagate DHC crack because the F in the cracking plane is low in the longitudinal specimen, therefore, the K_{IH} is high.

The cracking plane of the longitudinal specimen consisted of a ductile matrix, which is not susceptible to a DHC because $F_L = 0.03$, according to the concept shown in Fig. 13. This means that the material in this direction is very tough from the aspect of DHC, at least. Otherwise, the applied stress at the crack tip region by loading would have been greater than that of the yield stress of the longitudinal specimen. This is the reason why there is no K_{IH} result from the 0° specimen in Figs. 7 and 11.

The trend lines in Fig. 11 can be used to estimate the K_{IH} for any notch or crack which is tilted from the axial–radial plane of the pressure tube, although the results in Fig. 11 are obtained in purely from a Mode I condition. If the F for the cracking plane and the cracking direction can be determined, then the K_{IH} value for the flaws can be estimated, under the assumption that the crack or flaw propagates or extends along their plane at least.

The K_{IH} values should have a certain range of scatter due to material to material variations. However, since the most important application of K_{IH} would be for a flaw assessment of operating components, the minimum values may have a potential for a conservatism for a safe operation of a nuclear reactor.

5. Conclusions

The K_{IH} of the cantilever beam (CB) specimen with the highest F appeared to be the lowest K_{IH}, ~9 MPa $\sqrt{m}$, whereas that with the lowest F was over 20 MPa $\sqrt{m}$ at 250 °C. The K_{IH} in the radial direction decreased linearly with F for the cracking plane, and this is consistent with the results reported earlier. The texture dependence of K_{IH} in the Zr–2.5%Nb CANDU pressure tube material can be explained properly by the rule of a mixture using a model proposed earlier. It is demonstrated that

there are two different trends of K_{IH} according to the cracking direction. It is concluded that the K_{IH} is determined predominantly by F for the cracking plane and subsequently by the cracking direction. The trend of the texture dependence of K_{IH} can be used to estimate the K_{IH} in the radial direction for a notch or crack tilted in the axial direction.

Acknowledgments

This work has been carried out in the Reactor Materials Technology Development project as a part of the Nuclear R&D program funded by the Ministry of Science and Technology in Korea. The authors would like to acknowledge people working in building #375 in AECL-CRL for their help.

References

[1] C.E. Coleman, J.F.R. Ambler, Atomic Energy of Canada Ltd., Report, AECL-6250, 1979.
[2] S. Sagat, C.E. Coleman, M. Griffiths, B.J.S. Wilkins, in: Tenth International Symposium on Zirconium in the Nuclear Industry, ASTM STP 1245, ASTM, Philadelphia, 1994, p. 35.
[3] S.S. Kim, S.C. Kwon, Y.S. Kim, J. Nucl. Mater. 273 (1999) 52.
[4] C.E. Coleman, S. Sagat, K.F. Amouzouvi, in: 26th Annual Conference of Metallurgists Canadian Institute of Mining and Metallurgy, Atomic Energy of Canada Ltd., Report AECL-9524, 1987.
[5] C.E. Coleman, in: Fifth Conference on Zirconium in the Nuclear Industry, ASTM STP 754, ASTM, Philadelphia, 1982, p. 393.
[6] H. Huang, W.J. Mills, Metall. Trans. A 22A (1991) 2149.
[7] W.J. Mills, F.H. Huang, Eng. Fract. Mech. 39 (1991) 241.
[8] W.M. Evans, R.F. Gessner, J.G. Goodwin, Metall. Trans. 3 (1972) 2879.
[9] J.E. Winegar, Atomic Energy of Canada Ltd., Report, AECL-5626, 1977.
[10] S.S. Kim, Y.S. Kim, J. Nucl. Mater. 279 (2000) 286.
[11] S.S. Kim, Y.S. Kim, J. Korean Nucl. Soc. 32 (2000) 1.
[12] C.E. Coleman, B.A. Cheadle, C.D. Cann, J.R. Theaher, in: Eleventh International Symposium on Zirconium in the Nuclear Industry, ASTM STP 1295, ASTM, Philadelphia, 1996, p. 884.
[13] Y.S. Kim, S.C. Kwon, S.S. Kim, J. Nucl. Mater. 280 (2000) 304.
[14] L.A. Simpson, C.D. Cann, J. Nucl. Mater. 87 (1979) 303.
[15] A.C. Wallace, G.K. Shek, O.E. Lepik, in: Eighth International Symposium on Zirconium in the Nuclear Industry, ASTM STP 1023, ASTM, Philadelphia, 1989, p. 66.
[16] L.A. Simpson, C.W. Chow, in: Eighth International Symposium on Zirconium in the Nuclear Industry, ASTM STP 939, ASTM, Philadelphia, 1987, p. 579.
[17] C.K. Chow, L.A. Simpson, in: Case Histories Involving Fatigue and Fracture Mechanics, ASTM STP 918, ASTM, Philadelphia, 1987, p. 78.
[18] S.S. Kim, Y.S. Kim, K.S. Lim, Y.M. Cheong, K.N. Choo, in: Proceeding of the Korean Nuclear Society Fall Meeting, Korean Nuclear Society, Seoul, 1999, p. 259.